



# Application of the transition model with respect to the local roughness on RANS based aircraft icing code

Seungin Min<sup>1</sup>, Sejong Oh<sup>2</sup>, Kwanjung Yee<sup>1</sup>

<sup>1</sup> Seoul National University, Seoul, Korea

<sup>2</sup> Pusan National University, Busan, Korea

fafnir@snu.ac.kr, tazo@pusan.ac.kr, kjyee@snu.ac.kr

The influence of surface roughness over the ice-contaminated surface is a critical issue in numerical simulation of aircraft icing, since it affects the underlying physics of the frozen surface. Regarding the Reynolds-averaged Navier-Stokes model implementation, capturing the laminar-turbulent transition process is the fundamental aspects of the roughness prediction approach, resulting in a drastic change in the local shear which eventually affects roughness growth. To this end, this numerical investigation was performed to capture the inter-disciplinary process of the roughness growth in icing. The analytical roughness model was implemented on the RANS based aircraft icing code with an extension of the roughness amplification variable on the turbulent transition modeling. The study computed the analytical solution for local roughness from the force equilibrium equation of water film on the ice surface, considering the local flow and meteorological variables. The local roughness heights were embedded as a boundary condition on the roughness amplification equation, which delivers the impact of roughness to downstream, coupled with the local transition model to predict the transition onset on the iced airfoil. To validate the developed model, the roughness was compared with the experimental results. As the result, the model well predicts the trends according to the meteorological conditions. Then, the transition onset and resulting changes in the roughness height, skin friction and heat convection coefficient were demonstrated to describe the effect of roughness on the transition model. Finally, the qualitative discussion is made for the later time-scale ice accretion shape, and the necessity of the transition model considering local roughness was presented.

**Keywords—** *Aircraft icing, Surface roughness, Heat transfer, Turbulence model, Transition*

## I. INTRODUCTION

When an aircraft operates in cold and humid environments, super-cooled droplets in the atmosphere collide with the aircraft surface, resulting in ice accretion. Aircraft icing involves multi-scale shape deformation from gross geometric feature to microscopic surface roughness. This process involves with complex mass and heat transfer on the aerodynamic surface including heat convection and evaporation which are dominantly associated with temporal evolution of the ice formation. Considering that heat transfer strongly depends of the fluid properties and surface roughness, and aircraft icing affects these factors, precise prediction of local heat transfer coefficient can improve the accuracy of numerical solution for aircraft icing.

The heat transfer in aircraft icing is a critical issue in the initial stage of icing process, especially when the ice starts to get caught in the smooth clean surface [1, 2]. Icing induced

surface roughness is a major factor in the acceleration of the laminar-turbulent transition process and hence the changes in parameters related to freezing such as wall shear stress and heat transfer. Thus, the formation of roughness in the initial stage and consequent changes in the heat transfer coefficient have been studied in the past few years. P. E. Poinssatte et. al. [3] measured the local heat convection coefficient for the smooth NACA0012 airfoil, then P. E. Poinssatte and V. Fossen [4] measured the effect of roughness element on heat convection using artificial roughness. The local convective heat transfer intensity of the leading edge was obtained, which reached the peak at the stagnation point, and transition was accelerated by the leading edge roughness. M. F. Kerho and M. B. Bragg [5] conducted experimental study of the effects of distributed roughness located near the leading edge of an airfoil, and concluded that though roughness triggers the transition, the boundary layer does not reach a fully developed turbulent state immediately as previously assumed.

Currently, the heat transfer enhancement by the surface roughness is considered through numerical methods in aircraft icing codes. LEWICE [6], the aircraft icing code based on potential flow solution, separate the boundary layer transition point according to local roughness Reynolds number [7]. FENSAP-ICE [8], a coupled CFD/ice-accretion solver, used roughness the modified Spalart-Allmaras model to consider the surface roughness through flow analysis, and the transition region is predicted through trip term [9, 10].

However, these methods have several disadvantages in predicting changes in heat transfer due to surface roughness. Heat transfer analysis and transition position prediction through boundary layer theory and roughness Reynolds number have difficulty predicting heat convection coefficient at the high Reynolds number. Also, the immediate growth of heat transfer due to roughness in this method is different from the actual phenomenon. For the Spalart-Allmaras model used in the RANS-based Aircraft icing code, the transition position is predicted through the coefficients used in the trip term, but this requires a priori or educated guess. Due to the limitations of the existing numerical methodology, the aircraft icing simulation does not model the physical properties such as initial surface roughness and corresponding changes in the transition acceleration and heat transfer. This is as one reason of failing to simulate the important features of aircraft icing such as ice horns or ice formations on the ice surface under freezing conditions.

In this study, to take account of local surface roughness induced transition, we implemented the correlation based

transition model [7] based on the Shear Stress Transport (SST) model [11]. The effect of surface roughness on laminar-turbulent transition roughness effect parameter with transport equation is used [12]. For the roughness prediction, an advanced roughness model that can consider local roughness coupled with three-dimensional RANS-based aircraft icing code is proposed. To model the time-dependent surface roughness height, the analytical solution for the water film and bead height was determined from the governing equation of the SWIM model [8]. Parametric analysis was performed on the roughness height obtained by applying the roughness model. The effect of the roughness element on the heat convection coefficient and ice shape is also presented. In the current model, the surface roughness height follows the physical tendency of the experiments. The heat convection coefficient was changed by the surface roughness, but the ice shape was partially improved.

## II. METHODOLOGY

### A. Surface Roughness in Aircraft Icing

The surface roughness continuously changes from the beginning of the ice formation process according to the amount of water on the surface, the volume of the droplets, and the air force. Hansmann and Turnock [13] observed qualitative changes in the surface roughness on iced cylinder through a high-speed camera. They demonstrated that the water film was formed around the stagnation point of the cylinder. Subsequently, as shown in Fig. 1, it is divided into a water rivulet flow, and coagulated into water beads. Hansmann and Turnock [13] also qualitatively demonstrated that surface changes are affected by gravity, surface tension, and aerodynamic forces.

This change in surface roughness is clearly distinguished as the icing shape progresses. Shin [1], and Anderson and Shin [2] observed the characteristics of the surface roughness developed when icing occurred. He divided the surface of the aircraft into three stages: smooth region, rough region, and feather region. Shin [1] measured the surface roughness and measured the surface roughness of approximately 0.28–0.79 mm in the rough region initially formed. This affects the formation of the boundary layer thickness and thus the surface troposphere, which ultimately affects the shape and size of ice formation. In this study, the force equilibrium relation was

adopted to calculate the surface roughness, and the model was validated by comparing to the experiments with reference to the studies above.

### B. Roughness modeling

Herein, the surface roughness model assumes that the surface state is classified by the amount of the water on the surface. The concept was proposed by Fortin[14] and divides the surface state into a (1) film, (2) rivulet, and (3) bead state depending on the amount of water on the local surface. In this study, in order to apply this concept to the RANS equation based code, the amount of water was calculated through film thickness and the roughness height was computed through the force equation acting on each state.

At the initial stage of icing, water droplets in the air are attached to the aircraft surface in the form of stationary beads after impact. As icing proceeds, the water beads coalesce to grow, and beads over a certain size begin to move in the rivulet or film. Thus, the surface roughness varies with time; however, because the present code assumes a quasi-steady state, the numerical modeling of the transient state is limited. Therefore, the current model computes the roughness height for each time step and calculates the final shape by reflecting the effect of the roughness through interactions with the thermodynamic module. To calculate the surface roughness height, the current model divides the surface state into beads, rivulets, and films. The surface roughness model consists of four steps as follows. First, the  $h_{\text{bead}}$  and  $h_{\text{film}}$  are calculated by the surface condition according to the icing time. Then, calculate the force equation for the bead state. If the external force of the force equation is smaller than the surface tension, it is assumed to be a bead state, else it would be assumed to be rivulet or smooth water film region.

#### (1) Roughness height calculation

The surface roughness value of each state is derived from the mass conservation equation of the thermodynamic model of Eq. (1).

$$\rho_w \left\{ \frac{\partial h_f}{\partial t} + \nabla(h_f U_f) \right\} = \dot{m}_{\text{imp}} - \dot{m}_{\text{ice}} \quad (1)$$

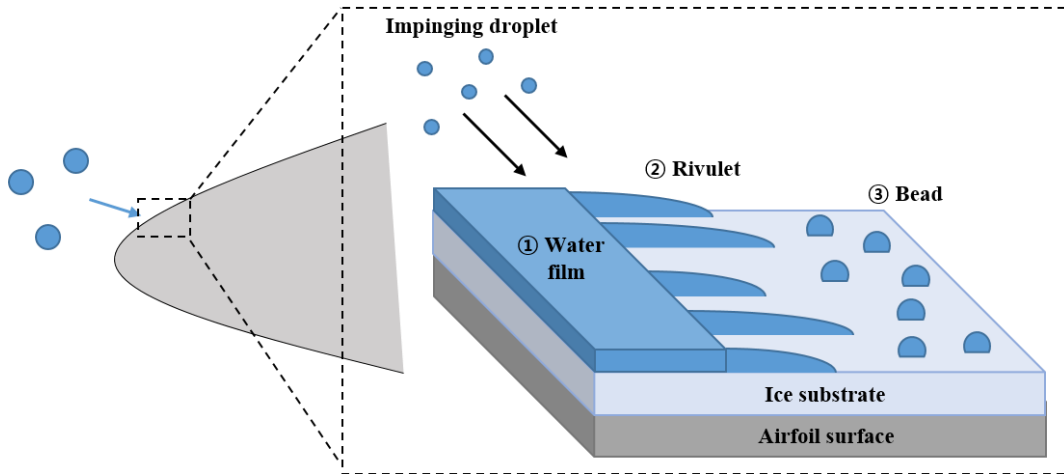


Fig. 1. Surface state change on the iced airfoil surface

The convection term is split into the incoming and outgoing water film flow mass of the control volume; subsequently, the equation above can be expressed as the following Eq. (2)

$$\rho_w \frac{\partial h_f}{\partial t} = \dot{m}_{imp} + \dot{m}_{in} - \dot{m}_{ice} - \dot{m}_{out} \quad (2)$$

At the bead state, the  $\dot{m}_{out}$  term can be expressed as zero because water does not flow out; thus, the surface roughness in the water droplet state can be expressed by the following Eq. (3). In this case,  $f_{shape}$  is a shape variable, assuming that the shape of the water drop is spherical, where  $\theta_c$  is the average contact angle of the bead.

$$h_b = \frac{1}{f_{shape}} \frac{1}{\rho_w} (\dot{m}_{imp} + \dot{m}_{in} - \dot{m}_{ice} - \dot{m}_{out}) \Delta t \quad (3)$$

$$f_{shape} = \sqrt{\frac{\theta_c - \sin \theta_c \cos \theta_c}{2 \sin \theta_c}} \quad (4)$$

## (2) Force equilibrium on the surface roughness

For the computed roughness height, gravitational and aerodynamic forces acting as the external force, with the surface tension acting as the reacting force are calculated as shown in Eq. (5)

$$F_{\sigma_w} = \rho_b g V_b + \tau_w A_b + \int \frac{dp}{dx} dV \quad (5)$$

At the bead state, the surface tension force equilibrates with the external force. When the external force exceeds the surface tension, the bead flows as a rivulet or a water film. The separation of the water film into a rivulet is determined by the magnitude of the force acting on the water film. Gravity, flow shear stress, and pressure act as external forces, as well as water droplets. The force equation for water film appears similarly as Eq. (5). When the external force acting on the water film is less than the surface tension, only a part of the water film flows; thus, it changes into a rivulet. Based on Eq. (6), the surface state is divided into a water film and a rivulet.

$$\sigma_w (1 - \cos \theta_c) = \frac{1}{2} \rho_w \left\{ \frac{\tau_w}{\mu_w} y - \frac{y^2}{\mu_w} \left( \frac{dp}{dx} + \rho g \right) \right\}^2 \quad (6)$$

## C. Effect of Surface Roughness on Aircraft Icing Code

In this study, a model considering the variation in surface roughness with time was applied to a RANS-based aircraft icing code [15]. The aircraft icing code consists of four modules: sequentially computing the aerodynamic force, droplet trajectory, thermodynamics, and shape deformation. Although aircraft icing is an inherently unsteady phenomenon lasting from a few to tens of minutes, a quasi-steady state was assumed for computational efficiency. To consider the impact of shape change owing to icing, a multishot method that divides the total icing time into several steps to account for the ice accretion as a function of time was used. The model was built in OpenFOAM™ [16], an open-source code.

Surface roughness transition owing to ice accretion induces changes in viscous effects associated with relative motion between the fluid and the surface. As the RANS equation focuses on the mean flow properties, the application of an adequate turbulence model considering the effect of roughness is required. In the case of a general turbulence model, since the analysis for both smooth surface and rough surface is required, correlation based transition model [7] with roughness effect transport equation [12] was used.

While original Shear Stress Transport (SST) model [11] directly takes account of surface roughness through the boundary condition for the turbulent kinetic energy and the dissipation rate [17], the Langtry-Menter model [7] lacks the ability to deliver effect of roughness on transition point [12]. Then, roughness amplification variable ( $A_r$ ) is additionally adopted as shown in Eq. (7)

$$\frac{\partial(\rho A_r)}{\partial t} + \frac{\partial(\rho U_j A_r)}{\partial x_j} = \frac{\partial}{\partial x_j} \left[ \left( \mu + \frac{\mu_t}{\sigma_f} \right) \frac{\partial A_r}{\partial x_j} \right] \quad (7)$$

The  $A_r$  transport equation are determined through the wall boundary condition as the function of sand grain roughness ( $k_s$ ), as shown in Eq. (8).  $k^+$  is non-dimensional sand grain-roughness. For the smooth wall region, the boundary condition for  $A_r$  is set as zero gradient boundary condition.

$$A_r|_{wall} = C_{r1} k^+ \quad (8)$$

The roughness variable  $A_r$  triggers the transition process by increase the local momentum thickness Reynolds number. This is accomplished through modification of production term in Eq. (10) of transport equation of transition onset momentum thickness Reynolds number ( $\widetilde{Re}_{\theta_t}$ ) as shown in Eq. (9). The  $F_{A_r}$  function includes the roughness variables and defined as the Eq. (11) and  $b$  is the blending function.

$$\frac{\partial(\rho \widetilde{Re}_{\theta_t})}{\partial t} + \frac{\partial(\rho U_j \widetilde{Re}_{\theta_t})}{\partial x_j} = P_{\theta_t} + \frac{\partial}{\partial x_j} \left[ \Gamma_{\theta_t} \frac{\partial \widetilde{Re}_{\theta_t}}{\partial x_j} \right] \quad (9)$$

$$P_{\theta_t, rough} = c_{\theta_t} \frac{\rho}{t} [(Re_{\theta_t} - \widetilde{Re}_{\theta_t})(1 - F_{\theta_t}) - b F_{A_r}] \quad (10)$$

$$F_{A_r} = \begin{cases} c_{r2} (A_r)^3 & : A_r < C_{A_r} \\ c_{r3} (A_r - C_{A_r}) + c_{r2} C_{A_r}^3 & : A_r \geq C_{A_r} \end{cases} \quad (11)$$

$$b = \left[ \frac{1}{2} \sin \left( \frac{\pi}{155} \widetilde{Re}_{\theta_t} - \frac{97\pi}{155} \right) + \frac{1}{2} \right]^2 \quad (12)$$

The roughness also affects the boundary condition for the specific dissipation rate ( $\omega$ ), proposed by the Wilcox [17]. Since both smooth and rough region is take considered, each boundary condition is presented as follows.

$$\omega_{smooth} = 10 \frac{6\nu}{\beta(\Delta y)^2} \quad \text{with } \beta = 0.09 \text{ at } y = 0 \quad (13)$$

$$\omega_{rough} = \frac{\mu_{\tau}^2 S_r}{\nu} \quad \text{with} \quad \mu_{\tau} = \sqrt{\frac{\tau_{wall}}{\rho_{wall}}} \quad \text{at} \quad y = 0 \quad (14)$$

Where  $S_r$  is dependent on the non-dimensional  $k^+$  value.

$$S_r = \begin{cases} \left(\frac{50}{k^+}\right)^2 & \text{if } k^+ \leq 25 \\ \frac{100}{k^+} & \text{if } k^+ > 25 \end{cases} \quad (15)$$

The surface roughness increases the size of the turbulent viscosity. Turbulent viscosity is calculated through turbulence model. This affects the thermal conductivity as shown in Eq. (16).

$$k_{eff} = \rho c_p \left( \frac{\nu}{Pr} + \frac{\nu_{turb}}{Pr_{turb}} \right) \quad (16)$$

The convective heat transfer coefficient, which is an important parameter of icing shape determination, is calculated from the thermal conductivity and the temperature gradient calculated in the aerodynamic module. Because the amount of icing is determined by the heat exchange at the surface, the increase in the convective heat transfer coefficient with increasing turbulent thermal conductivity affects the accuracy of the analysis.

$$h_{cv} = -k_{eff} \frac{\partial T}{\partial n} \left( \frac{1}{T_{sur} - T_{\infty}} \right) \quad (17)$$

Convective heat transfer balances the latent heat of solidification into the air and appears as the source term of the energy equation of the thermodynamic module [8]. Therefore, the surface roughness from the present model changes the heat convection coefficient through the turbulence model, which in turn influences the ice shape by the energy equation of the thermodynamic solver.

The surface roughness model that simulates the physical phenomena on the surface is applied to RANS based aircraft icing code. With taking account of physical plausibility, considering the unsteady change of the surface roughness requires huge amount of computation power due to its size and time step. Therefore analytical solution which can be applied to a quasi-steady assumption is derived for numerical efficiency. The predicted surface roughness is applied to the modified turbulent model of the RANS equation, which influences the flow field, wall shear stress, and heat convection.

### III. RESULT AND DISCUSSION

In this section, the ice thickness of the simulation with the current transition model and distributed roughness model applied are presented. First, the model was validated through comparison with the measured roughness height. Subsequently, the heat convection coefficient, which are physical parameters of the model application, are compared with result when fully turbulent model is applied instead of transition model. The ice thickness are presented to demonstrate the improvement of the model. The test model is

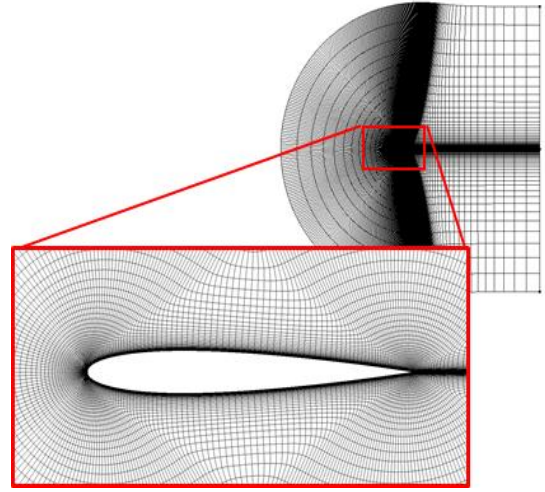


Fig. 2 NACA 0012 airfoil grid

the two-dimensional NACA0012, and the chord length is 0.5334 m. The mesh is the C-type grid, as shown in Fig. 2. The non-dimensional distance of the first cell is taken to be approximately  $y^+ = 1$ . The case are presented in Table I [18].

TABLE I. Test case matrix

	Case A	Case B
Airfoil	NACA 0012	
Angle of attack (°)	0	
Airspeed (m/s)	95.3	
$T_{total}$ (°C)	-2.3	-2.7
LWC (g/m <sup>3</sup> )	0.58	0.65
MVD (μm)	53.2	61.5
$\Delta T$ (sec)	97.2	86.7

#### A. Surface Roughness in Aircraft Icing

The surface roughness model that simulates the physical phenomena on the surface is applied to RANS based aircraft icing code. With taking account of physical plausibility, considering the unsteady change of the surface roughness requires huge amount of computation power due to its size and time step. Therefore analytical solution which can be applied to a quasi-steady assumption is derived for numerical efficiency. The predicted surface roughness is applied to the modified turbulent model of the RANS equation, which influences the flow field, wall shear stress, and heat convection.

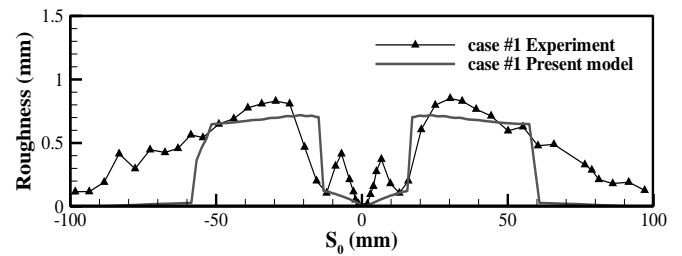


Fig. 3. Surface roughness distribution

The current model computes the surface roughness based on the force equilibrium on the surface, and thus distributed roughness is computed as shown in Fig. 3. The numerical roughness height, as shown in the experiment, forms a smooth zone consisting of a water film in the stagnation region near the leading edge, followed by a rough zone where the roughness grows rapidly. This trend is related to the laminar-turbulence transition. When the transition occurs, the wall shear stress is increased and the water film on the surface is accelerated. Therefore, in the laminar region with relatively low heat convection and high water content, a smooth zone appears, and a rough zone appears after the transition. The region where the roughness suddenly decreases in a numerical result is a rime ice region where impinging water is all freezing, and has limitations in simulating the current model of roughness as a force equilibrium equation for surface water.

In this section, we validate the roughness model by comparing the experimental value. The present model confirms that the surface condition which greatly affects the flow characteristics in the initial icing process affects the smooth zone and the rough zone similarly to the experimental value.

### B. Heat convection

The present aircraft icing code applies the roughness height to the turbulent model to compute the modified turbulent viscosity, and thus heat convection coefficient. In this section, the heat transfer coefficient is validated compared to the experimental result conducted by P. E. Poinsatte [3] and V. Fossen [4]. Fig. 4 and Fig. 5 represents the Frossling number representing the Nusselt number ( $Nu = h_{cv}L/\kappa$ ) divided by square root of freestream Reynolds number about the smooth and rough NACA0012 airfoil. The surface temperature and the ambient temperature were 35°C and -6.7°C. Reynolds number was 1.2million.

As in Fig. 4, Frossling number computed from present transition model and Spalart-Allmaras model for the smooth airfoil are compared with experimental results. It shows that near leading edge both model predicts the similar peak value, while result of Spalart-Allmaras model shows higher value at the downstream region. Generally, the laminar to turbulent transition in smooth airfoil occurs at the rear region of the airfoil, but a fully turbulent model such as Spalart-Allmaras does not exhibit this characteristic. However, present model

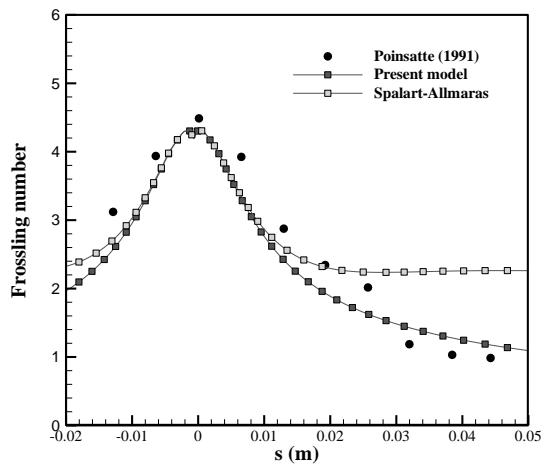


Fig. 4 Frossling number for smooth NACA 0012

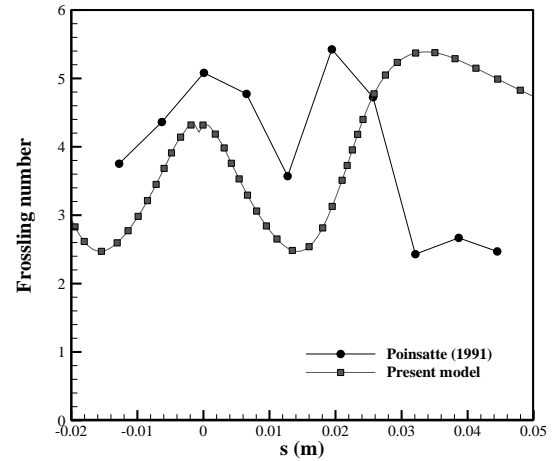


Fig. 5 Frossling number for rough NACA 0012

follows the experimental result, concluding that laminar region is well predicted through the model.

Fig. 5 shows the result of rough airfoil case with densely distributed 1mm height semi-sphere roughness. For the numerical analysis, the roughness value are simply embedded as 1mm. The numerical results follows the trends of the experiment. Near the leading edge, both results shows the laminar characteristics, and as flow pasts about 2%-chord region, it forces the flow to transition in the leading edge. This results are similar with the findings of M. F. Kerho and M. B. Bragg [5] that it was near impossible to force the flow to transition in the leading 2%-chord region of the airfoil no matter how large the roughness element were near the stagnation point.

Fig. 6 shows the roughness induced transition model and the Frossling number when Spalart-Allmaras is applied to case B. This result shows the difference of each model. In the case of roughness-induced transition, laminar-turbulence transition occurs due to the roughness of the laminar flow of the leading edge, as shown in the previous experimental study. On the other hand, for the Spalart-Allmaras model, the flow is assumed to be Fully Turbulent, which results in a high heat transfer rate from the leading edge. The difference in heat transfer rate according to this turbulence model is discussed in detail in the next section by comparing the ice thickness.

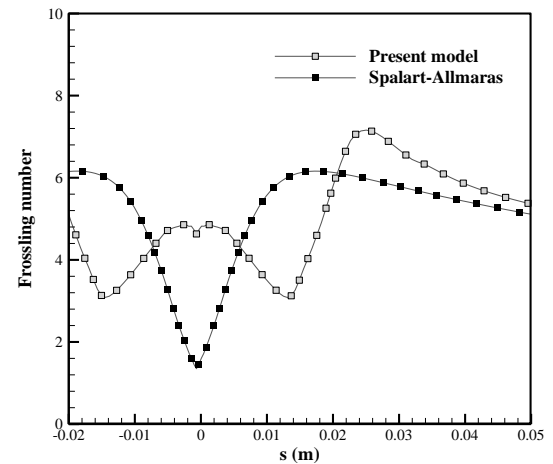


Fig. 6 Frossling number comparison

### C. Ice thickness

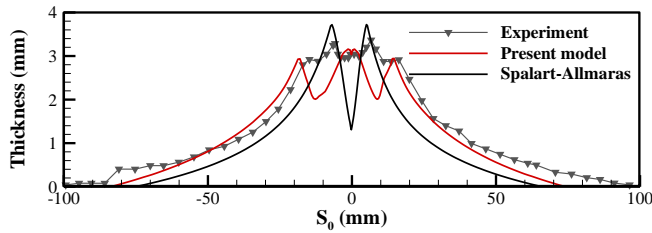


Fig. 7 Ice thickness comparison

Fig. 7 represents the ice thickness when applying the present transition model with roughness consideration and Spalart-Allmaras model. Both results show different trends in the stagnation region near the leading edge. This follows the trend of the heat transfer rate shown in Fig 6.

In the case of the present transition model, starting from laminar flow at the leading edge, the ice thickness decreases before the transition occurs and then increases again after the transition. There is some mismatch from that of the plateau form near the leading edge in the experimental results, because the current transition model is more rapid than the actual laminar-turbulence transition in the numerical solution.

In the case of Spalart-Allmaras, two peaks occur near the leading edge. The Spalart-Allmaras model is a fully turbulent model with the highest heat convection coefficient immediately past the leading edge. According to the above results, when the turbulence model considering the roughness induced transition is applied, the shape differs from ordinary Spalart-Allmaras model in the stagnation region. This is because the heat convection coefficient affected by the turbulence model is dominant in the aircraft icing process.

Roughness-induced transitions were considered to predict the overall shape better than the results obtained using the conventional Spalart-Allmaras. There is propensity of ice accretion thickness follows the heat convection coefficient, which has the dominant effect on the ice accretion rate. From this perspective, considering the surface roughness distribution and its transition can help improve the accuracy of the freezing shape prediction.

However there are some considerations, Depending on the characteristics of the transition model currently used and the heat convection calculation method at the leading edge, the ice form tends to be calculated to be small for the laminar-turbulence transition region. The better results can be obtained if the modeling of the transition area according to the icing roughness and the heat convection calculation in the corresponding area are improved.

### IV. CONCLUSION

The transition model considering the roughness effect was implemented into a RANS-based aircraft icing code. The motivation of this study is to solve the physical plausibility of the local roughness prediction by dividing smooth and rough zone then consider roughness effect on transition process, therefore predict heat convection and ice accretion shape precisely. The concept of the roughness model was to distinguish three surface states based on the force equilibrium relation on the surface, and to compute the roughness height.

Along with the advances in the methodology, this study showed the limitations of the existing models, and it predicted an improvement in the ice shape with different tendency of heat convection. It was confirmed that the physical model for the roughness height was reliable, and the physical characteristics which scarcely considered through other aircraft icing code were applied to the RANS-based aircraft icing code. However, there were some limitations of implementing this model alone to the icing code to precisely compute the ice shape. Since transition model with roughness consideration consists of 5 equations, computation efficiency declines. Also, further investigation is required for some physical loopholes to extend present method to other applications, such as complicated 3D shapes. Nevertheless, this study has laid the basis for a heuristic approach for a more advanced aircraft icing code development based on physical phenomena.

### ACKNOWLEDGMENT

This work was supported by the Korea Agency for Infrastructure Technology Advancement(KAIA) grant funded by the Ministry of Land, Infrastructure and Transport (Grant 18CHTR-C128889-02)

### REFERENCES

- [1] J. Shin, "Characteristics of surface roughness associated with leading edge ice accretion," NASA TM-106459, 1994.
- [2] D. N. Anderson, and J. Shin, "Characterization of Ice Roughness from Simulated Icing Encounters," NASA TM 107400, 1997.
- [3] P. E. Poinatte, G. V. Fossen, J. E. Newton, and K. J. DeWitt., "Heat transfer measurements from a smooth NACA 0012 airfoil," *Journal of Aircraft*, vol. 28, no. 12, pp. 892-898, 1991.
- [4] P. E. Poinatte, G. V. Fossen, and K. J. DeWitt., "Roughness effects on heat transfer from a NACA 0012 airfoil," *Journal of Aircraft*, vol. 28, no. 12, pp. 908-911, 1991.
- [5] M. F. Kerho, and M. B. Bragg, "Airfoil boundary-layer development and transition with large leading-edge roughness," *AIAA journal*, vol. 35, no. 1, pp. 75-84, 1997.
- [6] G. A. Ruff, and B. M. Berkowitz, "Users' Manual for the NASA Lewis Ice-Accretion Prediction Code (LEWICE)," NASA CR 185129, 1990.
- [7] F.R. Menter, R. Langtry, and S. Volker, "Transition modelling for general purpose CFD codes," *Flow, turbulence and combustion*, vol. 77, no. 1-4 pp. 277-303, 2006.
- [8] H. Beaugendre, F. Morency, and W. G. Habashi, "FENSAP-ICE's three-dimensional inflight ice accretion module ICE3D," *Journal of Aircraft*, vol. 40, no. 2, pp. 239-247, 2003.
- [9] P. R. Spalart, and S. Allmaras, "A one-equation turbulence model for aerodynamic flows," *30th aerospace sciences meeting and exhibit*, p. 439, 1992..
- [10] P. R. Spalart, and B. Aupoix, "Extensions of the Spalart-Allmaras Turbulence Model to Account for Wall Roughness," *International Journal of Heat and Fluid Flow*, vol. 24, no. 4, pp. 454-462, 2001.
- [11] F. R. Menter, "Two-equation eddy-viscosity turbulence models for engineering applications," *AIAA journal*, vol. 32, no. 8, pp. 1598-1605-, 1994.
- [12] P. Dassler, D. Kozulovic, and A. Fiala, "An approach to modelling the roughness-induced boundary layer transition using transport equations," *European Congress on Computational Methods in Applied Sciences and Engineering*, 2012.
- [13] R. J. Hansman, and S. R. Turnock, "Investigation of Surface Water Behavior During Glaze Ice Accretion," *Journal of Aircraft*, vol. 25, no. 2, pp.140-147, 1989.
- [14] G. Fortin, A. Ilinca, J. L. Laforte, and V. Brandi, "New roughness computation method and geometric accretion model for airfoil icing," *Journal of Aircraft*, vol. 41, no. 1, pp. 119-127, 2004.
- [15] C. Son, S. Oh, and K. Yee, "Development of 2nd generation ice accretion analysis program for handling general 3-D geometries,"

*Journal of Computational Fluids Engineering*, vol. 20, no.2, pp. 23-36, 2015.

- [16] OpenFOAM, “Open-source Field Operation and Manipulation,” *Software Package*, Ver. 2.2.0, 2011, <http://www.openfoam.com>.
- [17] B. Aupoix, “Wall Roughness Modelling with kw STT Model”, *10th International ERCOFTAC Symposium on Engineering Turbulence Modelling and Measurements*, 2014.
- [18] S. T. McClain, M. M. Vargas, and J. Tsao, “Characterization of Ice Roughness Variations in Scaled Glaze Icing Conditions,” *8th AIAA Atmospheric and Space Environments Conference*. 2016.